

Fracture Curve of a Thin-walled Tube in Torsion Test

WU JIE-QING

Department of Mechanics, Zhejiang University, Hangzhou, PRC

ABSTRACT

The torsion test of a thin-walled steel tube was used to find the shearing proportional limit τ_p and the yielding limit τ_s . More recently it has also been used to measure the ultimate strength τ_b and to draw a complete torque-angle ($M-\theta$) curve or a stress-strain ($\bar{\tau}-R_m\theta/l$) curve. In this paper, an analysis of the whole fracture process of the tube by means of a fracture curve is made. The whole $M-\theta$ curve actually contains two parts, the loading and the fracture curves. And the fracture curve further includes three sections, the convex, the straight and the concave portions. On the straight portion the nominal shearing stress τ_n is kept constant and the stress intensity factor of Mode II, K_{II} , varies. The starting point of this portion is available to calculate the critical value of K_{II} , K_{IIC} , which is about $0.7K_{IC}$ for steel. An approximate formula $K_{IC}:K_{IIC}:K_{IIC} = 1:0.8:0.7$ is established. Materials arbitrarily chosen in the test are 30Cr, 40Cr, 9SiCr and 45 carbon steels. Some related characteristics of crack propagation are also described.

KEYWORDS

Torque-angle curve; loading curve; stress-strain curve; strain parameter; proportional limit; yielding limit; ultimate strength; fracture curve; convex portion; stress intensity factor of Mode II; straight portion; concave portion; ultimate torque; fracture angle; step.

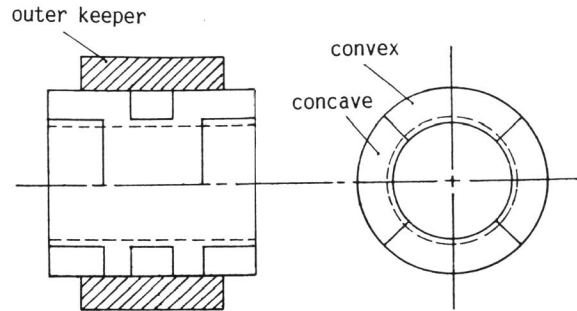


Fig. 1. Specimen schema

LOADING CURVE OF A THIN-WALLED TUBE

Fig.1 shows the tube specimen which has short gauge length so as to avoid buckling. An outer keeper added is for the purpose of keeping the coaxiality of the specimen during testing. Fig. 2 shows the typical torque-angle curve, in which OA is the loading curve and ABCDEFR the fracture curve. From the complete loading curve, a $\tau-R_m\theta/l$ curve may be deduced. Then the proportional limit τ_p , the yielding limit τ_s and the ultimate stress τ_b are easily determined. In addition, by equality of strains and by equality of stresses, there are two transformation formulas between two tubes with different sizes for the same material:

$$\frac{R_{m1}\theta_1}{l_1} = \frac{R_{m2}\theta_2}{l_2} \quad (1)$$

$$\frac{M_1}{(2\pi)R_{m1}^2 t_1} = \frac{M_2}{(2\pi)R_{m2}^2 t_2}$$

Where M is the applied torque, R_m the mean radius and t the thickness. Using (1), the M- θ curve for a large tube may be obtained from that for a small one. But there exists only one $M/(2\pi R_m^2 t) - R_m\theta/l$ curve or $\tau - R_m\theta/l$ curve which can represent the shearing stress distribution along the radius of a torsion shaft, solid or hollow, loaded to elasto-plastic stage (Wu Jie-Qing, 1988). $R_m\theta/l$ is a shearing strain parameter, which was first suggested by the author and which can be used to show both small and large shearing strains.

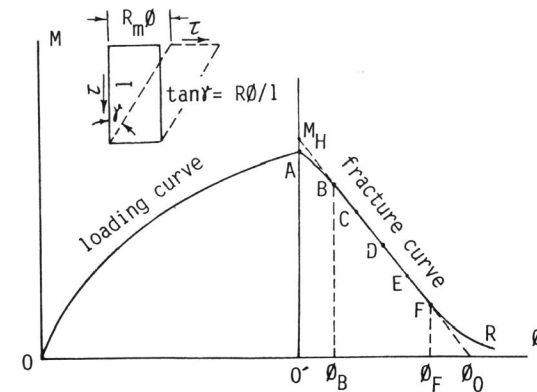


Fig. 2. Complete M- θ curve.

When strain is small, $R_m\theta/l \approx \gamma$. For a solid circular torsion specimen or shaft, $r\theta/l$ is proportional to r, the radial point distance. (1) may be called the second transformation formulas as compared with the first ones (Wu Jie-Qing, 1985)

$$\frac{R_1\theta_1}{l_1} = \frac{R_2\theta_2}{l_2} \quad (1')$$

$$\frac{M_1}{R_1^3} = \frac{M_2}{R_2^3}$$

which is for solid specimens and from which a sole $M/R^3 - R\theta/l$ curve is obtained for both small specimen and large shaft.

FRACTURE CURVE

If the straight portion is extended, it intersects the vertical axis at M_H and the horizontal axis at θ_0 which is measured from the new origin O' . The equation of the straight portion is

$$M = -\frac{M_H}{\theta_0} \theta + M_H \quad (2)$$

where $M_H (> M_A)$ is the ideal ultimate torque and θ_0 the ideal fracture angle. The length of the penetrated crack 2a may reasonably be expressed as

$$2a = kR_m\theta \quad (3)$$

where k is a constant to be determined. When $\theta = \theta_0$, then $2a = 2\pi R_m$. After sub-

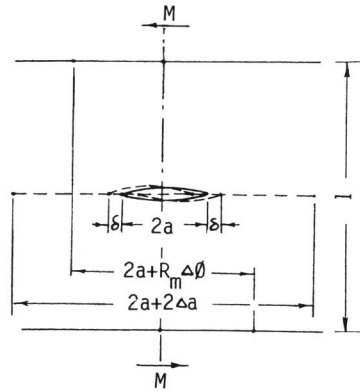


Fig. 3. Schema showing $2\Delta a > R_m \Delta \phi > 2\delta$.

stituting in (3),

$$k = \frac{2\pi}{\phi_0} \quad (4)$$

By (4), (3) becomes

$$2a = 2\pi R_m \frac{\phi}{\phi_0} \quad (3')$$

Due to $\phi_0 < 2\pi$ for the short gauge length of the tube, $k > 1$. And from (2), the steepness M_H/ϕ_0 or $(M_H/2\pi)k$ is proportional to k . From (3), we obtain

$$k = \frac{2\Delta a}{R_m \Delta \phi} \quad \text{or} \quad \frac{\Delta a}{\Delta \phi} = \frac{\pi R_m}{\phi_0} \quad (= \text{cons.}) \quad (5)$$

Therefore $2\Delta a$, the increment of the crack length, is greater than $R_m \Delta \phi$, the increment of circumferential relative displacement between two tube ends which is still much greater than 2δ , see fig.3. The tip speed $\frac{\Delta a}{\Delta \phi}$ is constant.

On the other respect, the test of a thin-walled tube is an important method to measure K_{IIC} . But the torsion tube with a crack of length $2a$ is just the same case as a repeated section of an infinite plate in shear, as shown in fig. 4. Thus

$$\tau_\infty = \frac{M}{2\pi R_m^2 t} \quad (6)$$

The nominal shearing stress τ_n in the tube ligament is given by

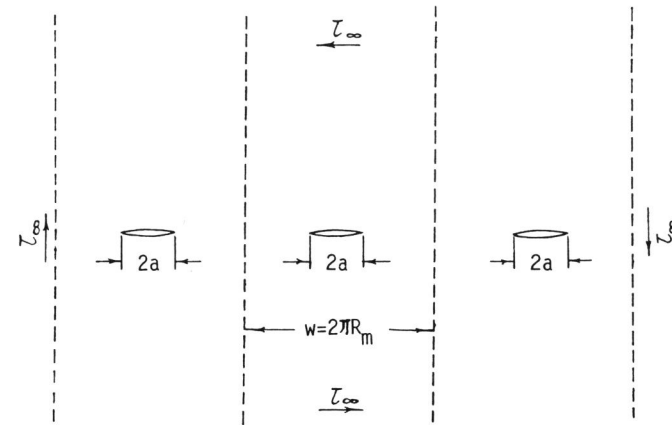


Fig. 4. Infinite plate in shear with cracks in line.

$$\tau_n = \frac{M}{(W-2a)R_m t} \quad (7)$$

where $W = 2\pi R_m$. Then from (6) and (7)

$$\tau_\infty = \left(1 - \frac{2a}{W}\right) \tau_n \quad (8)$$

which shows $\tau_n \geq \tau_\infty$.

If the curvature of the convex portion is neglected, (7) becomes

$$\tau_n = \frac{M_H}{2\pi R_m^2 t} \quad (9)$$

which is τ_n when $a = 0$. However, for the points on the portion BC, if putting (2) into (7) and using relation (3'), we still have (9). That is, along the straight portion, τ_n is a constant which can be calculated by (7) or (9). See table 1(a) and (b). It should be noted that the constancy of τ_n deduced is based on (3) or (3').

The expression of K_{II} is

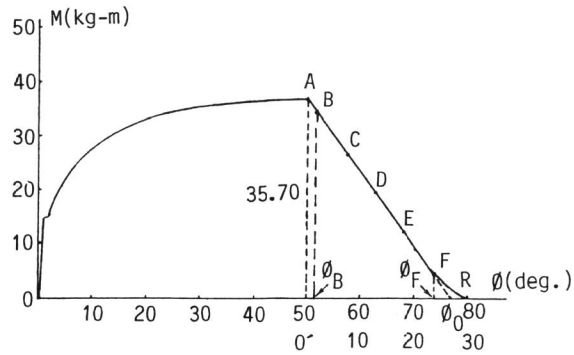


Fig. 5(a). Loading and fracture curves (30Cr steel specimen No 1)

Table 1(a). Data for points on straight portion (30Cr steel specimen No 1)

Points	M(kg-m)	θ (deg.)	2a(mm)	K_{II} (kg/mm ^{3/2})	τ_n (kg/mm ²)
B	33.00	2.25	6.48	194.33	66.27
C	26.30	7.25	20.87	285.92	66.19
D	20.00	12.00	34.54	297.36	66.27
E	12.60	17.50	50.38	260.38	65.92
F	4.00	24.00	69.09	154.60	66.27

Note: $D_m=24.74$ mm, $t=0.565$ mm, $l=10.20$ mm, $M_A=35.70$ kg-m, $\tau_b = \frac{M_A}{(2\pi R_m^2 t)} = 65.72$ kg/mm², $\theta_0=27.00^\circ$, $k=13.33$.

$$K_{II} = YZ\sqrt{\pi a} \quad (10)$$

where

$$Y = \sqrt{\tan(\pi a/W) / (\pi a/W)} \quad (11)$$

In order to calculate K_{IIC} , we take a_B for a , B is the starting point of the straight portion, at which the small penetrated central crack is completely formed and begins to propagate. Since a_B is always much smaller than W , Y is taken as 1. Then we write

$$K_{IIC} = \tau_{\infty B} \sqrt{\pi a_B} \quad (12)$$

where, by (6),

$$\tau_{\infty B} = \frac{M_B}{2\pi R_m^2 t} \quad (13)$$

Fig. 5(a) and table 1(a) show the $M-\theta$ curve and the calculated results respectively for 30Cr steel, specimen No 1. And fig. 5(b) and table 1(b) are given for specimen No 2. We have the mean values: $K_{IIC}=199.17$ kg/mm^{3/2}, $\tau_n = 65.41$ kg/mm².

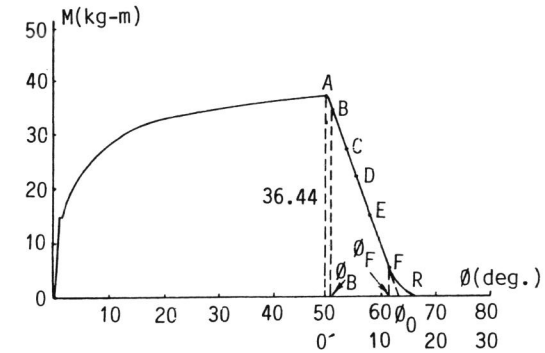


Fig. 5(b). Loading and fracture curves (30Cr steel specimen No 2)

Table 1(b). Data for points on straight portion (30Cr steel specimen No 2)

Points	M(kg-m)	θ (deg.)	2a (mm)	K_{II} (kg/mm ^{3/2})	τ_n (kg/mm ²)
B	32.90	1.25	7.69	204.00	65.14
C	27.17	3.25	20.00	278.33	65.34
D	22.00	5.00	30.77	293.71	65.04
E	15.60	7.25	44.61	274.76	65.40
F	4.50	11.00	67.69	156.27	62.27

mean 64.64

Note: $D_m=24.74\text{mm}$, $t=0.583\text{mm}$, $l=10.20\text{mm}$, $M_A=36.44\text{kg-m}$, $\tau_b=65.01\text{kg/mm}^2$, $\phi_0=12.63^\circ$, $k=28.50$.

Table 2. K_{IC} , K_{IIIC} , K_{IIC} of steels.

Steel	$K_{IC}(\text{kg/mm}^{3/2})$	$K_{IIIC}(\text{kg/mm}^{3/2})$	$K_{IIC}(\text{kg/mm}^{3/2})$	$K_{IC}:K_{IIIC}:K_{IIC}$
30Cr	280.79	229.22	199.69	1:0.816:0.711
40Cr	310.00	252.45	227.95	1:0.814:0.735
9SiCr	278.68	236.40	196.05	1:0.848:0.704
45#	209.94	177.02	144.27	1:0.843:0.687

K_{IC} and K_{IIIC} for 30Cr steel which have already been measured are $K_{IC}=280.79\text{kg/mm}^{3/2}$, $K_{IIIC}=229.22\text{kg/mm}^{3/2}$ (Wu Jie-Qing, 1984, 1983). Therefore

$$K_{IC} : K_{IIIC} : K_{IIC} = 1 : 0.816 : 0.711$$

or approximately

$$K_{IC} : K_{IIIC} : K_{IIC} = 1 : 0.8 : 0.7 \quad (14)$$

K_{IC} , K_{IIIC} and K_{IIC} have also been measured for other kinds of steel, 40Cr, 9SiCr, and 45 carbon steels. Table 2 shows that the approximate formula (14) is well established. Values of K_{IIC} found by (14) are conservative as compared with those obtained from S ($K_{IIC}=0.96K_{IC}$, for $\nu=0.3$) and G ($K_{IIC}=K_{IC}$) criteria.

ADDITIONAL DISCUSSION

Here only the convex portion (thickness affected zone) and the concave portion (step affected zone) are discussed. The convex portion in fact corresponds to the enlarge of a surface crack from the outside to the inside of the tube to form a perfect penetrated crack at point B. If the tube thickness is approaching zero, the convex portion finally becomes a part of the straight portion. Ratio ϕ_B/ϕ_0 is adapted to assess the thickness influence. See fig. 6 (a). Tips of a crack travel around in opposite directions and do not meet each other at one point usually. See fig. 6(b). A step is to be formed and the corresponding concave portion FR in fracture curve appears. The dashed, elongated portion from point F is corresponding to no step. The ligment length at F is given by

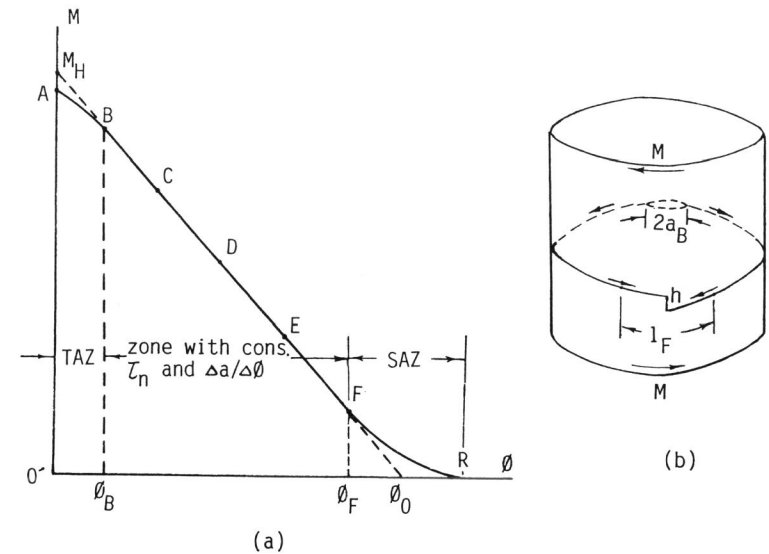


Fig. 6. (a). Three portions and corresponding zones; (b). Propagating path and step.

Table 3. Values of ϕ_B/ϕ_0 , $\frac{\phi_F-\phi_B}{\phi_0}$, $\frac{\phi_0-\phi_F}{\phi_0}$.

Specimen No (30Cr)	t (mm)	k	ϕ_B (deg.)	ϕ_F (deg.)	ϕ_0 (deg.)	$2a_B$ (mm)	l_F (mm)	$\phi_B/\phi_0(\%)$	$\frac{\phi_F-\phi_B}{\phi_0}(\%)$	$\frac{\phi_0-\phi_F}{\phi_0}(\%)$
1	0.565	13.33	2.25	24.00	27.00	6.49	8.64	8.3	80.6	11.1
2	0.583	28.50	1.25	11.00	12.63	7.69	10.03	9.9	77.2	12.9

Note: $\frac{\phi_B}{\phi_0} = \frac{2a_B}{2\pi R_m}$, $\frac{\phi_F-\phi_B}{\phi_0} = 1 - \frac{2a_B+l_F}{2\pi R_m}$, $\frac{\phi_0-\phi_F}{\phi_0} = \frac{l_F}{2\pi R_m}$.

$$l_F = 2\pi R_m \left(1 - \frac{\phi_F}{\phi_0}\right) \quad (15)$$

When $\phi_F=\phi_0$, then $l_F=0$ and the step height $h=0$. One step shows that there exists only one penetrated crack. The specimen breaks into two at last at the step with slant fracture faces. It should be noted that, on the fracture surface, the initial cracking point is always in the opposite position to the step in a diameter.

CONCLUSIONS

1. The loading curves for tubes of different sizes can be transformed from one to another. A loading curve with changed scales on axes represents a stress-strain ($\tau - R_m \theta / l$) curve.
2. The starting point of the straight portion in a fracture curve is used to calculate K_{IIC} . An approximate formula (14) is available for steel.
3. τ_n is the same for points on the straight portion, so is $\Delta a / \Delta \theta (= \pi R_m / \theta_0)$. τ_n may be regarded to be τ_b .
4. The convex portion with the corresponding thickness affected zone shows the process in which a small initial surface crack develops into a complete penetrated crack.
5. The concave portion shows a step to be formed in the fracture surface.
6. If the loading speed increases, a steeper straight portion and a smaller θ_0 will result. Compare fig.5(a) and (b).

REFERANCES

- Wu Jie-Qing (1983), A Simple Method for Measuring K_{IIC} of Ductile Metals and Its Applications, Proceedings of ICF International Symposium on Fracture Mechanics, pp.591-601, Science Press, Beijing.
- Wu Jie-Qing (1984), Some Improvements on the Ring-cracked Tensile Specimen for Measuring K_{IC} of Ductile Metals, Proceedings of ICF6, Vol.7, pp.216-219, Pergamon Press.
- Wu Jie-Qing (1985), Transformation of Torque-Angle Diagrams in Torsion Test for Round Bars of Ductile Metals with Different Diameters, Physical Testing and Chemical Analysis, Vol.21, No.5, pp.31-32, Shanghai. (in Chinese)
- Wu Jie-Qing (1988), Calculation of Shearing Stress Distribution for a Large Torsional Shaft Loaded to and Unloaded from Elasto-plastic Stage, Proceedings of ICES-88(in Atlanta), Chap.29, Springer-Verlag.